Cell. Mol. Biol. (ISSN: 1165-158X)

Journal Homepage: www.cellmolbiol.org

Cellular and Molecular Biology

Original Article

Circ_0006220 (circ-TADA2A) accelerates prostate cancer cell malignant behaviors through miR-520f-3p/CDCA7 axis

Zijin Wan, Gang Liu*

Department of Urinary Surgery, Ganyu District People's Hospital of Lianyungang City, Lianyungang, Jiangsu 222100, China

Article Info

Article history:

Received: February 06, 2024
Accepted: May 10, 2024
Published: July 31, 2024

Use your device to scan and read the article online

Abstract

Prostate cancer (PCa) belongs to a prevailing neoplasm globally. Circular RNAs (circRNAs) are critical regulators in various tumors, but the role of circRNAs in PCa is obscure. In this research, a circRNA derived from the TADA2A gene (hsa_circ_0006220) was high-expressed in PCa tissues along with cell lines. Elevated Circ-0006220 expression was also related to PCa poor prognosis. Besides, circ-0006220 accelerated PCa cells malignant behaviors in vitro; it also promoted PCa tumor growth together with metastasis in vivo. Moreover, circ-0006220 competed with the Cell Division Cycle Associated 7 (CDCA7) for binding to miR-520f-3p. Circ-0006220 sponged miR-520f-3p to regulate CDCA7 expression, thereby promoting PCa cell proliferation, migration, invasion, along with metastasis. All above data suggested that circ-0006220 may be a worthy target for PCa therapeutics.

Keywords: Prostate cancer, circ-0006220, miR-520f-3p, Migration, Invasion, Epithelial-to-mesenchymal transition.

1. Introduction

Prostate cancer (PCa) ranks the second most frequent kind of cancer globally, along with about one million per annum [1, 2]. As the global population grows and ages, by 2030, the annual incidence and death rates of PCa are expected to exceed 1.5 million and 499,000, respectively [3]. Hence, it is necessary to probe diagnostic and prognostic biomarkers in PCa.

Circular RNAs (circRNAs) are a class of single-stranded RNAs with their 30 and 50 ends covalently linked into a loop [4, 5]. Previous literatures have unveiled that a variety of circRNAs contribute to pathological process of PCa [6-8]. Circ-0006220 is a novel circRNA, and its location was mapped to chr17: 35800605-35800763 and formed by TADA2A; It was recently shown that circ-TADA2A is explicitly over-expressed in PCa [9]; nevertheless, its biological potential has not been defined.

Cell division cycle-associated protein 7 (CDCA7), its location is on chromosome 2q31, and it can encode a nuclear protein including 371 amino acids [10]. CDCA7 was first identified in Myc-transfected fibroblasts and is up-regulated in multiple human cancers [11]. Besides, CDCA7 is a c-Myc-responsive gene that engages in cancer tumorigenesis [10]. In addition, many reports have shown that CDCA7 is highly expressed in many cancers [11-16]. Recently, reports have shown that CDCA7 is aberrantly upregulated in PCa, proposing the potentiality of being a novel marker for PCa diagnosis and prognosis [17, 18].

Previous reports demonstrated that miRNA-30a and 30d inhibit non-small cell lung cancer via CDCA7 [19] and that miR-30a and d regulate CDCA7 to enhance putative resistance to pemetrexed therapy [20]. MiR-520f has been documented to be engaged in regulating cancer progression [21-23]; it has been found to be low-expressed in PCa [24], and its expression is promoted in response to radiation therapy of PCa patients [25-27]. All above findings strongly mirror the vital role of circ-0006220, miR-520f, and CDCA7. Therefore, our research aimed to scrutinize the latent mechanism of circTADA2A concerning the miR-520f/CDCA7 axis.

2. Materials and methods

2.1. Patients' samples

From March 2020 to May 2022 through surgery, PCa as well as paired normal tissue samples from 37 patients were gathered before the procedure for the study. All patients provided informed consent, and the study was approved by the Institutional Review Board of Ganyu District People's Hospital of Lianyungang City.

* Corresponding author.
E-mail address: LiuG663@163.com (G. Liu).
Doi: http://dx.doi.org/10.14715/cmb/2024.70.7.12

2.2. Cell culture

Procell (Wuhan, China) provided human PCa cell lines (PC-3, DU 145, 22RV1, as well as VCaP) together with normal human prostate epithelial cells (RWPE-1). DMEM (#PM150210B, Procell) was adopted for culturing VCaP and DU 145 cells. 22RV1 cells were cultivated in RPMI-1640 medium (#PM150145, Procell). PC-3 cells were cultivated in F-12 medium (#PM150810B, Procell). All cell mediums were added with 10% FBS and grown at 37°C in 5% CO_2 atmosphere.

2.3. Cell transfection

Experiments were implemented in triplicate. PLKO.1-puro together with pLVX-EF1a plasmid vectors were provided by HonorGene (Changsha, China). A shRNA construct targeting circ-0006220 and the corresponding negative control were cloned into PLKO.1-puro. The sequences encoding circ-0006220, CDCA7, along with negative control were cloned into pLVX-EF1a. The miR-520f-3p mimics together with miR-520f-3p inhibitor were provided by RIBOBIO (Guangzhou, China). Plasmids transfection was implemented using Lipofectamine 3000 (#L3000008, Solarbio).

2.4. RNA extraction and qRT-PCR

PCa cells were harvested by centrifugation at 4°C, and the total RNA was extracted at room temperature (20–25°C) using TRIzol reagent (#15596026, Invitrogen). Subsequently, cDNA was generated by means of the OneStep PrimeScript R miRNA cDNA Synthesis Kit (#D350A, Takara, China). The RT analysis of gene expression was utilized using SYBR Green I fluorescence method for PCR detection. The utilized primer sequences are as follows: E-cadherin, F-5'-GCTGGACCGAGAGAGTTTCC-3', R-5'-CAAAATCCAAGCCCGTGGTG-3'; Vimentin, F-5'-CGGGAGAAATTGCAGGAGGA-3', R-5'-AAGGTCAAGACGTGCCAGAG-3'; Snail, F-5'-TCGGAAGCCTAACTACAGCGA-3', R-5'-AGATGAGCATTGGCAGCGAG-3'; circ-0006220, F-5'-CCCTGCTGAACCTGAAAC-3', R-5'- CACTCCTCCTTGGTCTTG-3'; miR-520f-3p, F-5'-GTGCTTCCTTTTAGAGGG-3', R-5'-GAACATGTCTGCGTATCTC-3'; CDCA7, F-5'-GGGTGGCGATGAAGTTTCCA-3', R-5'-GGGGATGTCTTCCACGGAAC-3'; β-actin, F- 5'-CTCGCCTTTGCCGATCC-3', R-5'-TTCTCCATGTCGTCCCAGTT-3'. $2^{-\Delta\Delta Ct}$ method was implemented to determine gene expression in each sample. Experiments were implemented three times.

2.5. RNase R digestion

Experiments were implemented three times. Three units of RNase R (#R7092L, Beyotime, Shanghai, China) per 1 mg circ-0006220 were added for 15 min. qRT-PCR was implemented to test circ-0006220 levels normalized to β-actin.

2.6. Western blot

Experiments were implemented three times. Separation of protein samples was implemented by polyacrylamide gel electrophoresis and then shifted onto PVDF membranes, and then sealed in 5% non-fat milk for one hour, and then treated with primary antibodies containing CDCA7, E-cadherin, Snail, as well as vimentin (all from Abcam, Shanghai, China) at 4°C overnight. Afterwards, membranes were washed thrice and then treated with goat anti-rabbit secondary antibody (Abcam).

2.7. Cell counting kit-8 assay

In brief, 5×10^3 cells/well were planted into 96-well plates, followed by adding Cell Counting Kit-8 solutions (#C0037, Beyotime). We used a microplate reader (Thermo Fisher Scientific) and determined the OD reading at 450 nm. Assays were implemented in triplicate.

2.8. Colony formation assay

Assays were implemented thrice. Cells were planted in 6-well plates for fourteen days of incubation, followed by fixation with methanol along with staining with 0.1% crystal violet (#G1063, Solarbio, Beijing, China), and clones were counted.

2.9. Ethynyl-2-deoxyuridine (EdU) incorporation assay

Assays were implemented thrice. An EdU incorporation assay (#ab222421, Abcam) was adopted to assess cell proliferation. Briefly, after cell transfection, 100 ml of 50 mM EdU/well was added into cells and incubated for two hours at 37°C. Fluorescence microscopy was used for observation.

2.10. Transwell migration and invasion assays

Experiments were implemented in triplicate. Transwell™ chambers were adopted, and coated with or without Matrigel. Cells in a 200 mL serum-free medium were put into the upper chambers. 600 mL complete medium was placed into the bottom chambers. Forty-eight hours later, the upper chamber was removed. The migrated cells were fixed and stained, followed by counting using a BX53 Olympus fluorescence microscope.

2.11. RNA fluorescent in situ hybridization (FISH)

Experiments were implemented in triplicate. The circ-0006220 probe was designed by RIBOBIO and labeled with FAM fluorescent dye. RNA FISH (RIBOBIO) was implemented. Images were taken using a confocal laser-scanning microscope (ZEISS).

2.12. Dual-luciferase reporter assay

Experiments were implemented in triplicate. Before being cloned into the pRL-TK plasmid (#D2760, Beyotime) vector, circ-0006220 wild type, or CDCA7 wild type, which contained designed miR-520f-3p binding sites or mutant sequences with deleted target sites were constructed and amplified. Subsequently, HEK293T cells were co-transfected with luciferase plasmids, together with miR-520f-3p mimics or controls. Renilla and firefly luciferase activity was detected via the Dual-Luciferase Reporter Assay System (Promega).

2.13. Tumor xenograft implantation in nude mice

Experiments were implemented in triplicate. BALB/c nude mice (male, 4 weeks old) were obtained from Junke Biological Co., LTD (Nanjing, China). Animal studies were implemented following the guidelines of the animal ethical committee of Ganyu District People's Hospital of Lianyungang City. 1×10^7 22RV1 cells/ml transfected with sh-circ-0006220 or sh-NC were subcutaneously injected into the right flank of the mice. Tumors were measured every seven days post-injection, and the tumor volumes

were calculated (as a rotational ellipsoid). The mice were sacrificed four weeks later and recorded tumors weights.

2.14. Immunohistochemical analysis

Experiments were implemented in triplicate. The representative specimens stained with H&E were performed by immunohistochemical detection with antibodies against CDCA7 and Ki67 (Abcam).

2.15. Statistical analysis

The difference was evaluated as appropriate by unpaired Student's t-test (comparisons between two groups) or one-way ANOVA followed by post hoc Bonferroni test (comparisons between multiple groups). Overall survival rates were assessed using the log-rank test and Kaplan–Meier survival curves, and Pearson's correlation analysis verified the relation between circ-0006220 and CDCA7. The relation between circ-0006220 expression and the clinicopathological features of PCa patients was analyzed by Fisher's exact test. Data were expressed as mean ± standard deviation. $P < 0.05$ was significant. SPSS version 19.0 software was applied for statistical analyses.

3. Results

3.1. Circ-0006220 is up-regulated in PCa and increases PCa cell growth

Circ-0006220 (circ-TADA2A) exhibits high expression in PCa cells [9]. The circ-0006220 sequence was revealed in circBase database (Figure 1A). Then, it was discovered that circ-0006220 expression was related to lymph-node metastasis (Table 1). Besides, circ-0006220 was highly expressed in PCa tumor tissues (Figure 1B). Likewise, circ-0006220 expression was elevated in the PCa cell lines, including 22RV1, DU 145, VCaP, as well as PC-3, relative to normal prostate epithelial cell line RWPE-1 (Figure 1C).

After RNase R treatment, circ-0006220 structure presented more resistance to RNase R relative to TADA2A (Figure 1D). Kaplan–Meier analysis displayed patients with high circ-0006220 expression were accompanied with low survival time (Figure 1E).

Next, influences of circ-0006220 on PCa cell proliferation were probed. First, the efficacy of the sh-circ-0006220 plasmid as well as the circ-0006220 expression plasmid in PCa cells was tested respectively (Figure 1F). Then, cell functional assays unveiled that silencing circ-0006220 inhibited PCa cell growth (Figure 1G, H, J) while overexpressing circ-0006220 promoted PCa cell proliferation (Figure 1G, I, K).

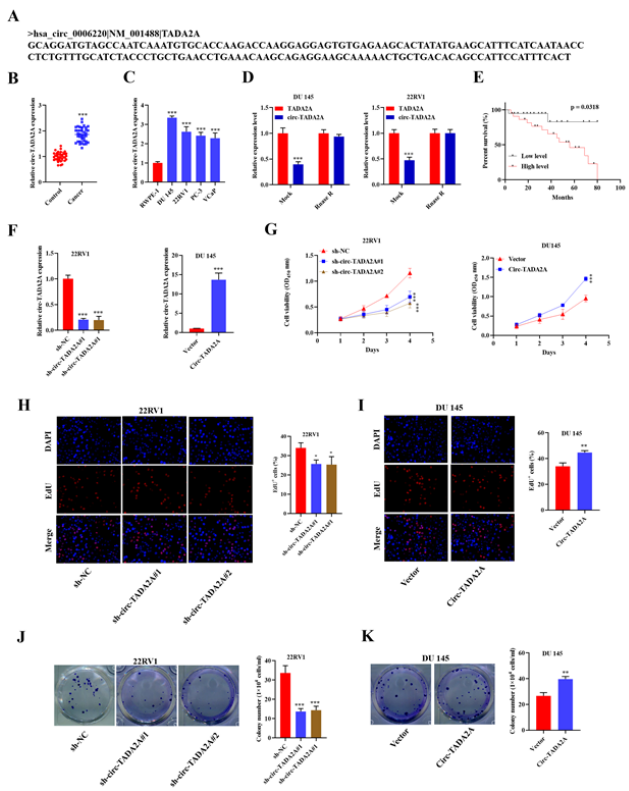

Fig. 1. Circ-0006220 expression in PCa and increases PCa cell growth. (A) Circ-0006220 sequence from circBase database. (B) circ-0006220 expression in PCa tissues. (C) qRT-PCR tested circ-0006220 expression in PCa cell lines. (D) RNase R digestion. (E) Relation between circ-0006220 and the overall survival of PCa patients from Kaplan–Meier survival curve with the log-rank test. (F) Transfection efficiency of circ-0006220 shRNAs and circ-0006220 overexpression vector. (G–K) PCa cell proliferation was analyzed by CCK-8, EdU, together with colony formation experiments. *p < 0.05, **p < 0.01, ***p < 0.001.

Table 1. The correlation between circ-0016068 expression and clinicopathological characteristics of PCa patients.

Feathers	Number	High	Low	P-value
All cases	37	19	18	
Age (Years)				0.7463
<65	20	12	8	
≥65	17	9	8	
Gleason score				0.7431
≥7	16	7	9	
<7	21	11	10	
Lymph-node metastasis				*0.0167
Yes	27	21	6	
No	10	3	7	
Tumor stage				0.5119
T1-T2	13	7	6	
T3-T4	24	10	14	

*P < 0.05 was statistical difference.

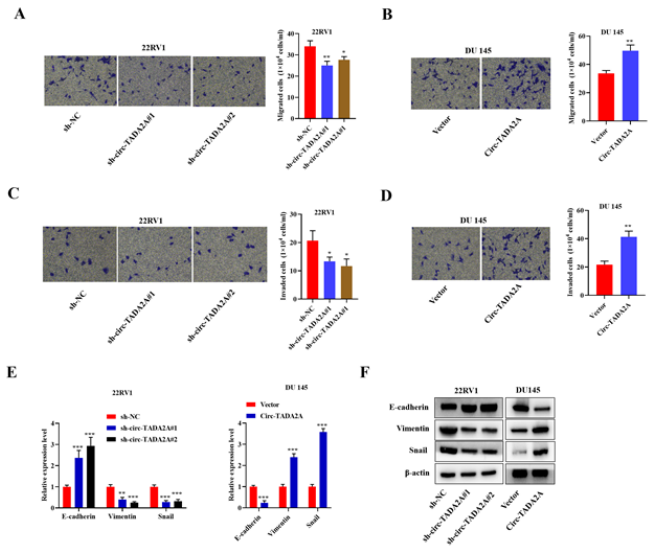

Fig. 2. Circ-0006220 promotes migration, invasion and EMT in PCa cells. (A, B, C, D) Silenced circ-0006220 on PCa cells migration and invasion were tested by transwell assay (scale bar = 100 mm). (E, F) Expression of EMT markers in PCa cells upon circ-0006220 depletion was assessed by (E) qRT-PCR and (F) Western blot. *p < 0.05, **p < 0.01, ***p < 0.001.

3.2 Circ-0006220 elevates PCa cell migration, and invasion along with EMT

Furthermore, circ-0006220 knockdown hindered PCa cell migration and invasion (Figure 2A, C), but overexpressed circ-0006220 exerted the opposite effects (Figure 2B, D).

In addition, circ-0006220 depletion elevated E-cadherin expression, while lessened vimentin together with snail expression in PCa cells, but circ-0006220 up-regulation exhibited the opposite effect in PCa cells (Figure 2E, F).

3.3 Circ-0006220 regulates CDCA7 expression via binding to miR-520f-3p

Based on RNA-FISH assay, circ-0006220 was discovered to be mainly located in the cytoplasm (Figure 3A). Former reports suggested that CDCA7 drove the initiation of PCa [17, 18]. Herein, a positive relation between the circ-0006220 and CDCA7 expression was observed in PCa tissues (Figure 3B). Moreover, knocking circ-0006220 down inhibited CDCA7 protein expression in PCa cells, and the inverse outcome was discovered upon circ-0006220 elevation (Figure 3C). CDCA7 was more highly expressed in PCa tissues than paired non-tumor tissue (Figure 3D).

Based on TargetScan and Circinteractome, miR-520f was confirmed to harbor putative binding sequences with both circ-0006220 and CDCA7 (Figure 3E). CDCA7 expression was elevated in the PCa cell lines (Figure 3F). Besides, miR-520f-3p was low-expressed in PCa tissues together with cell lines (Figure 3G, H).

Dual-luciferase reporter analysis results indicated that the luciferase intensities of wild-type CDCA7 and wild-type circ-0006220 were reduced by miR-520f-3p overexpression, but those of mutant-type CDCA7 and mutant-type circ-0006220 were not affected by miR-520f-3p mimics (Figure 3I).

Moreover, overexpressed miR-520f-3p reduced CDCA7 expression in PCa cells (Figure 3J). Besides, the repression of CDCA7 expression caused by circ-0006220

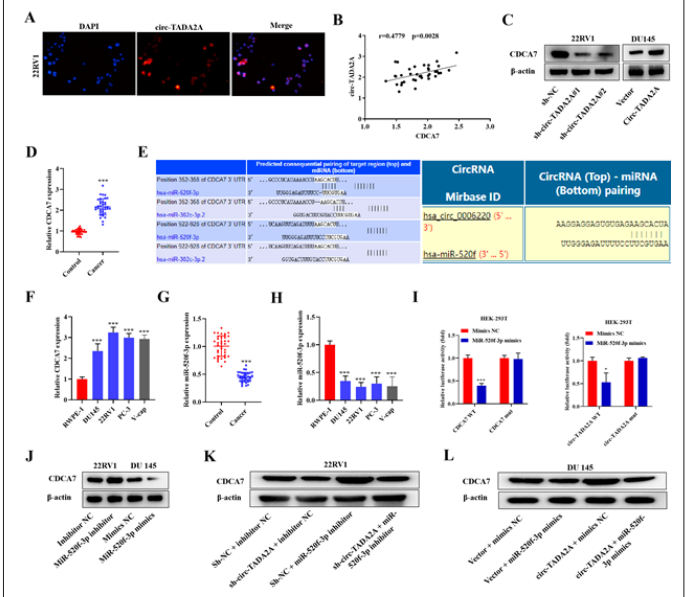

Fig. 3. Circ-0006220 elevates CDCA7 expression by binding to miR-520f-3p. (A) RNA-FISH determined subcellular localization of circ-0006220 in PCa cells. (B) Pearson's correlation coefficient of circ 0006220 and CDCA7 expression in PCa tissues. (C) CDCA7 expression in PCa cells upon circ-0006220 knockdown or overexpression by western blotting. (D) The level of CDCA7 in PCa tissues. (E) Bioinformatics analyses of TargetScan, and circinteractome. (F) CDCA7 expression in PCa cells. (G, H) MiR-520f-3p expression was tested in PCa tissues together with PCa cells. (I) Dual-luciferase reporter assay verified the combination of miR-520f-3p with CDCA7/circ-0006220. (J) CDCA7 expression in PCa cells was tested upon miR-520f-3p inhibition or elevation by western blot. (K) CDCA7 expression in PCa cells was determined by western blot in different groups. (L) Impacts of circ-0006220 elevation and miR-520f-3p overexpression on CDCA7 were assessed by western blot. *p < 0.05, ***p < 0.001.

silence was reversed by miR-520f-3p inhibition (Figure 3K). Meanwhile, overexpressing circ-0006220 that contained the MRE of miR-520f-3p abolished the reduced CDCA7 expression regulated by miR-520f-3p increase (Figure 3L).

3.4 Overexpression of CDCA7 offsets the effects of circ-0006220 on PCa cells

CDCA7 elevation rescued the reduced CDCA7 expression in circ-0006220 knockdown 22RV1 cells (Figure 4A). Moreover, elevated CDCA7 rescued the repressive proliferation caused by circ-0006220 depletion in PCa cells (Figure 4B, C). Likewise, CDCA7 elevation rescued the inhibited PCa cell migration and invasion upon circ-0006220 knockdown (Figure 4D, E).

3.5 Knockdown circ-0006220 represses PCa tumor growth and metastasis in vivo

Circ-0006220 reduction inhibited the tumor volume and weight of mice tumors (Figure 5A–B). Also, silenced circ-0006220 lessened CDCA7 expression together with EMT in the xenograft tumors (Figure 5C, D). Additionally, CDCA7 and Ki67 expression declined in PCa tumors when circ-0006220 was silenced (Figure 5E).

4. Discussion

PCa is the utmost frequent cancer diagnosed in men worldwide [28]. Although the course is indolent in most

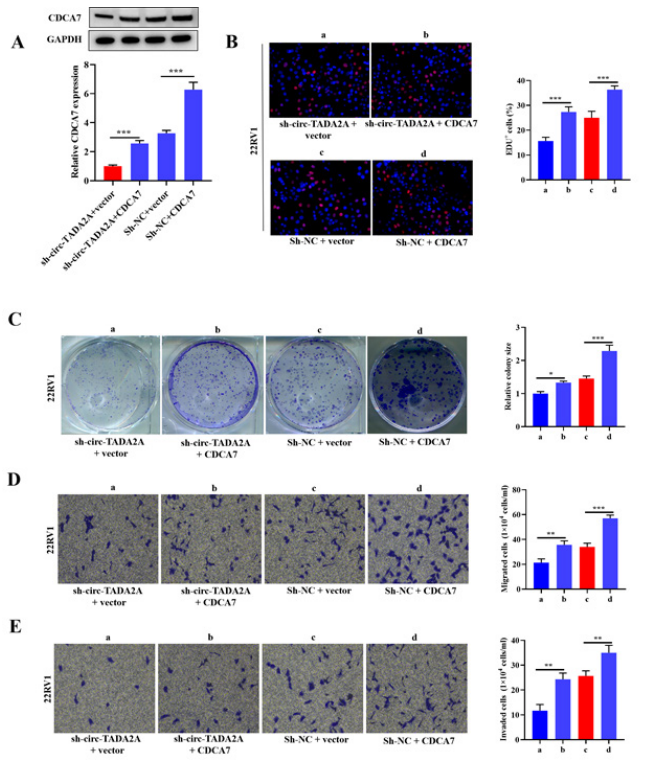

Fig. 4. CDCA7 elevation reverses the circ-0006220 silence-caused inhibited proliferation, migration and invasion of PCa cells. Rescue experiments were implemented in PCa cells transfected with sh-circ-TADA2A+vector, sh-circ-TADA2A+CDCA7, sh-NC+vector and sh-NC+CDCA7, respectively. (A) CDCA7 expression. (B, C) EdU together with colony formation assay. (D) Migration and (E) invasion of PCa cells. *p < 0.05, **p < 0.01, ***p < 0.001.

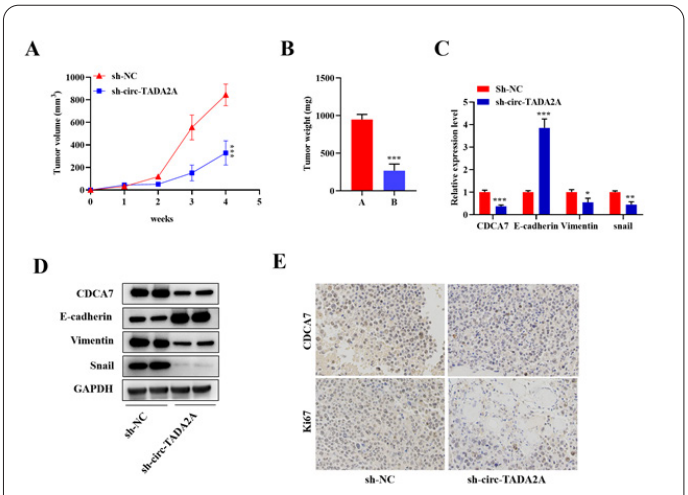

Fig. 5. Circ-0006220 promotes tumor growth and metastasis in vivo. (A) Tumor volumes after sh-circ-0006220 silence. (B) Tumor weights. (C, D) Expression of CDCA7 and EMT markers were tested after sh-circ-0006220 silence in vivo. (E) CDCA7 and Ki67 expression were tested after sh-circ-0006220 silence in vivo by immunohistochemical staining. *p < 0.05, **p < 0.01, ***p < 0.001.

cases, most patients with localized disease possess a high risk of recurrence along with metastasis. In spite of treatment, these patients often die from the disease [29, 30]. Hence, improved clinical diagnostic and therapeutic approaches to PCa are a fateful endeavor.

Emerging evidence displays that various circRNAs take part in physiological and pathological processes of tumors. CircRNAs modulate gene expression via distinct mechanisms [31], which can either drive or suppress tumorigenesis.

This study demonstrated that circ-0006220 levels were elevated in PCa tissues together with cell lines, and silenced circ-0006220 inhibited PCa cell growth, and invasion, along with migration in vitro. Besides, a positive relation between circ-0006220 expression and CDCA7 was found in PCa tumors, and inhibited circ-0006220 reduced CDCA7 expression. Moreover, both circ-0006220 and CDCA7 promoted the EMT of PCa and had putative binding sites of miR-520f-3p.

Former literatures demonstrated that miR-520f-3p inhibits gastric cancer progression [21], and hepatocellular carcinoma [22], and is a biomarker for lung cancer diagnosis [23]; but some literatures showed that miR-520f-3p reverses cancer EMT, obstructing cancer progression and inhibiting chemoresistance [32]. All above reports imply the potentials of miR-520f-3p may vary from cancer type. Here, miR-520f-3p levels were reduced in PCa tissues. MiR-520f-3p up-regulation declined CDCA7 levels in PCa cells. Furthermore, circ-0006220 silence decreased CDCA7 expression, while inhibited miR-520f-3p reversed CDCA7 levels.

In rescue experiments, up-regulated CDCA7 restored the suppressive proliferation, and migration, along with invasion of PCa cells upon circ-0006220 silence.

The present research had some limitations. It is essential to provide a larger sample size for investigating the clinical significance of circ-0006220 further. Broad spectrum target genes or miRNAs should be adopted for binding to circ-0006220. Also, the mechanism underlying the up-regulation of circ-0006220 in PCa should be investigated via further assays.

5. Conclusion

In conclusion, circ-0006220 acted as miR-520f-3p sponge to regulate CDCA7 that promoted PCa cell growth, migration, and invasion. Thus, our findings propound a novel foundation for probing the progression of PCa. In addition, these data implicated circ-0006220 may be a promising target for novel PCa therapeutics.

Conflict of interests

The authors declare no competing interests

Consent for publications

The author read and approved the final manuscript for publication.

Ethics approval and consent to participate

We have received approval from the Ethics Committee of Ganyu District People's Hospital of Lianyungang City.

Informed consent

We have received informed consent from the Ethics Committee of Ganyu District People's Hospital of Lianyungang City.

Availability of data and material

The data that support the findings of this study are available from the corresponding author upon reasonable request.

Authors' contributions

LG designed and supervised the study and revised the ma-

nuscript. WZ conducted the experiments, performed data analysis and drafted the manuscript.

Funding
Not applicable.

Acknowledgements
Not applicable.

References

1. Ferlay J, Shin HR, Bray F, Forman D, Mathers C, Parkin DM (2010) Estimates of worldwide burden of cancer in 2008: GLOBOCAN 2008. Int J Cancer 127: 2893-2917. doi: 10.1002/ijc.25516. PMID: 21351269.
2. Gnanapragasam VJ, Lophatananon A, Wright KA, Muir KR, Gavin A, Greenberg DC (2016) Greenberg. Improving Clinical Risk Stratification at Diagnosis in Primary Prostate Cancer: A Prognostic Modelling Study. PLoS Med 13: e1002063. doi: 10.1371/journal.pmed.1002063. PMID: 27483464.
3. Center MM, Jemal A, Lortet-Tieulent J, Ward E, Ferlay J, Brawley O, Bray F (2012) International variation in prostate cancer incidence and mortality rates. Eur Urol 61: 1079-1092. doi: 10.1016/j.eururo.2012.02.054. PMID: 22424666.
4. Gong GH, An FM, Wang Y, Bian M, Wang D, Wei CX (2018) Comprehensive Circular RNA Profiling Reveals the Regulatory Role of the CircRNA-0067835/miR-155 Pathway in Temporal Lobe Epilepsy. Cell Physiol Biochem 51: 1399-1409. doi: 10.1159/000495589. PMID: 30485839.
5. Zhang J, Zhang X, Li C, Yue L, Ding N, Riordan T, Yang L, Li Y, Jen C, Lin S, Zhou D, Chen F (2019) Circular RNA profiling provides insights into their subcellular distribution and molecular characteristics in HepG2 cells. RNA Biol 16: 220-232. doi: 10.1080/15476286.2019.1565284. PMID: 30614753.
6. Chen Y, Yang F, Fang E, Xiao W, Mei H, Li H, Li D, Song H, Wang J, Hong M, Wang X, Huang K, Zheng L, Tong Q (2019) Circular RNA circAGO2 drives cancer progression through facilitating HuR-repressed functions of AGO2-miRNA complexes. Cell Death Differ 26: 1346-1364. doi: 10.1038/s41418-018-0220-6. PMID: 30341421.
7. Feng Y, Yang Y, Zhao X, Fan Y, Zhou L, Rong J, Yu Y (2019) Circular RNA circ0005276 promotes the proliferation and migration of prostate cancer cells by interacting with FUS to transcriptionally activate XIAP. Cell Death Dis 2019 10: 792. doi: 10.1038/s41419-019-2028-9. PMID: 31624242.
8. Shen Z, Zhou L, Zhang C, Xu J (2020) Reduction of circular RNA Foxo3 promotes prostate cancer progression and chemoresistance to docetaxel. Cancer Lett 468: 88-101. doi: 10.1016/j.canlet.2019.10.006. PMID: 31593800.
9. Greene J, Baird AM, Lim M, Flynn J, McNevin C, Brady L, Sheils O, Gray SG, McDermott R, Finn SP (2021) Differential CircRNA Expression Signatures May Serve as Potential Novel Biomarkers in Prostate Cancer. Front Cell Dev Biol 9: 605686. doi: 10.3389/fcell.2021.605686. PMID: 33718350.
10. Prescott JE, Osthus RC, Lee LA, Lewis BC, Shim H, Barrett JF, Guo Q, Hawkins AL, Griffin CA, Dang CV (2001) A novel c-Myc-responsive gene, JPO1, participates in neoplastic transformation. J Biol Chem 276: 48276-48284. doi: 10.1074/jbc.M107357200. PMID: 11598121.
11. Cho H, Lim BJ, Kang ES, Choi JS, Kim JH (2009) Molecular characterization of a new ovarian cancer cell line, YDOV-151, established from mucinous cystadenocarcinoma. Tohoku J Exp Med 218: 129-139. doi: 10.1620/tjem.218.129. PMID: 19478469.
12. Albulescu R (2013) Elevated cyclin B2 expression in invasive breast carcinoma is associated with unfavorable clinical outcome. Biomark Med 7: 203. PMID: 23667945.
13. Cheng C, Zhou Y, Li H, Xiong T, Li S, Bi Y, et al (2016) Whole-Genome Sequencing Reveals Diverse Models of Structural Variations in Esophageal Squamous Cell Carcinoma. Am J Hum Genet 98: 256-274. doi: 10.1016/j.ajhg.2015.12.013. PMID: 26833333.
14. Jiménez-P R, Martín-Cortázar C, Kourani O, Chiodo Y, Cordoba R, Domínguez-Franjo MP, Redondo JM, Iglesias T, Campanero MR (2018) CDCA7 is a critical mediator of lymphomagenesis that selectively regulates anchorage-independent growth. Haematologica 103: 1669-1678. doi: 10.3324/haematol.2018.188961. PMID: 29880607.
15. Osthus RC, Karim B, Prescott JE, Smith BD, McDevitt M, Huso DL, Dang CV (2005) The Myc target gene JPO1/CDCA7 is frequently overexpressed in human tumors and has limited transforming activity in vivo. Cancer Res 65: 5620-5627. doi: 10.1158/0008-5472.Can-05-0536. PMID: 15994934.
16. Wang QL, Chen X, Zhang MH, Shen QH, Qin ZM (2015) Identification of hub genes and pathways associated with retinoblastoma based on co-expression network analysis. Genet Mol Res 14: 16151-16161. doi: 10.4238/2015.December.8.4. PMID: 26662407.
17. Brandão A, Paulo P, Teixeira MR (2020) Hereditary Predisposition to Prostate Cancer: From Genetics to Clinical Implications. Int J Mol Sci 21. doi: 10.3390/ijms21145036. PMID: 32708810.
18. Schumacher FR, Al Olama AA, Berndt SI, Benlloch S, Ahmed M, Saunders EJ et al (2018) Association analyses of more than 140,000 men identify 63 new prostate cancer susceptibility loci. Nat Genet 50: 928-936. doi: 10.1038/s41588-018-0142-8. PMID: 29892016.
19. Taguchi YH (2016) Identification of More Feasible MicroRNA-mRNA Interactions within Multiple Cancers Using Principal Component Analysis Based Unsupervised Feature Extraction. Int J Mol Sci 17. doi: 10.3390/ijms17050696. PMID: 27171078.
20. Hou J, Lambers M, den Hamer B, den Bakker MA, Hoogsteden HC, Grosveld F, Hegmans J, Aerts J, Philipsen S (2012) Expression profiling-based subtyping identifies novel non-small cell lung cancer subgroups and implicates putative resistance to pemetrexed therapy. J Thorac Oncol 7: 105-114. doi: 10.1097/JTO.0b013e3182352a45. PMID: 22134068.
21. Hong S, Bi M, Chen S, Zhao P, Li B, Sun D, Tai J (2016) MicroRNA-520f suppresses growth of gastric carcinoma cells by target ATPase family AAA domain-containing protein 2 (ATAD2). Neoplasma 63: 873-879. doi: 10.4149/neo_2016_606. PMID: 27565325.
22. Xu FF, Xie WF, Zha GQ, Chen HW, Deng L (2017) MiR-520f promotes cell aggressiveness by regulating fibroblast growth factor 16 in hepatocellular carcinoma. Oncotarget 8: 109546-109558. doi: 10.18632/oncotarget.22726. PMID: 29312628.
23. Zhou Y, Shen S (2019) MiR-520f acts as a biomarker for the diagnosis of lung cancer. Medicine (Baltimore) 98: e16546. doi: 10.1097/md.0000000000016546. PMID: 31348274.
24. Kumar P, Sharad S, Petrovics G, Mohamed A, Dobi A, Sreenath TL, Srivastava S, Biswas R (2016) Loss of miR-449a in ERG-associated prostate cancer promotes the invasive phenotype by inducing SIRT1. Oncotarget 7: 22791-22806. doi: 10.18632/oncotarget.8061. PMID: 26988912.
25. Josson S, Sung SY, Lao K, Chung LW, Johnstone PA (2008) Johnstone. Radiation modulation of microRNA in prostate cancer cell lines. Prostate 2008; 68: 1599-1606. doi: 10.1002/pros.20827. PMID: 18668526.
26. Konoshenko MY, Bryzgunova OE, Laktionov PP (2021) miRNAs and radiotherapy response in prostate cancer. Andrology 9: 529-545. doi: 10.1111/andr.12921. PMID: 33053272.

27. Labbé M, Hoey C, Ray J, Potiron V, Supiot S, Liu SK, Fradin D (2020) microRNAs identified in prostate cancer: Correlative studies on response to ionizing radiation. Mol Cancer 19: 63. doi: 10.1186/s12943-020-01186-6. PMID: 32293453.
28. Dess RT (2020) Treatment Intensification in High-Risk Prostate Cancer: Lessons From the TROG 03.04 RADAR Trial. Int J Radiat Oncol Biol Phys 106: 703-705. doi: 10.1016/j.ijrobp.2020.01.005. PMID: 32092344.
29. Kearns JT, Holt SK, Wright JL, Lin DW, Lange PH, Gore JL (2018) PSA screening, prostate biopsy, and treatment of prostate cancer in the years surrounding the USPSTF recommendation against prostate cancer screening. Cancer 124: 2733-2739. doi: 10.1002/cncr.31337. PMID: 29781117.
30. Teo MY, Rathkopf DE, Kantoff P (2019) Treatment of Advanced Prostate Cancer. Annu Rev Med 70: 479-499. doi: 10.1146/annurev-med-051517-011947. PMID: 30691365.
31. Lyu D, Huang S (2017) The emerging role and clinical implication of human exonic circular RNA. RNA Biol 14: 1000-1006. doi: 10.1080/15476286.2016.1227904. PMID: 27588461.
32. van Kampen JGM, van Hooij O, Jansen CF, Smit FP, van Noort PI, Schultz I, Schaapveld RQJ, Schalken JA, Verhaegh GW (2017) miRNA-520f Reverses Epithelial-to-Mesenchymal Transition by Targeting ADAM9 and TGFBR2. Cancer Res 77: 2008-2017. doi: 10.1158/0008-5472.Can-16-2609. PMID: 28209612.